Polymer Engineering & Science

WILEY | spe INSPIRING PLASTICS PROFESSIONALS

RESEARCH ARTICLE OPEN ACCESS

Thermoresistive Sensors Based on Eco-Friendly Carbon Dioxide-Derived Polymeric Poly(Cyclohexene)carbonate Loaded With Reduced Graphene Oxide and Carbon Black

Ane Martín-Ayerdi[1] | Luis Rubio-Peña[2] | Nikola Peřinka[1] | Sergio Merillas[1] | Itziar Oyarzabal[1,3] | José Luis Vilas-Vilela[1,4] | Pedro Costa[5,6] | Senentxu Lanceros-Méndez[1,3,5]

[1]BCMaterials, Basque Center for Materials, Applications and Nanostructures, UPV/EHU Science Park, Leioa, Spain | [2]Engineering School, University of Cadiz, Puerto Real, Spain | [3]IKERBASQUE, Basque Foundation for Science, Bilbao, Spain | [4]Innovative Macromolecular Materials Group (Imacromat), Physical Chemistry Department, Faculty of Science and Technology, University of the Basque Country UPV/EHU, Leioa, Spain | [5]Physics Centre of Minho and Porto Universities (CF-UM-UP), and Laboratory of Physics for Materials and Emergent Technologies, LapMET, University of Minho, Campus of Gualtar, Braga, Portugal | [6]IB-S Institute of Science and Innovation for Sustainability, Universidade do Minho, Braga, Portugal

Correspondence: Nikola Peřinka (nikola.perinka@bcmaterials.net) | Senentxu Lanceros-Méndez (senentxu.lanceros@bcmaterials.net)

Received: 10 June 2026 | **Revised:** 24 July 2026 | **Accepted:** 27 July 2026

Keywords: carbon dioxide | polycarbonate | sustainability | thermoresistivity

ABSTRACT

Carbon dioxide-derived polycarbonates (CO_2-PCs) present a sustainable alternative to standard bisphenol A polycarbonates (BPA-PCs), as they are synthesized from the reaction between epoxide and carbon dioxide (CO_2). In fact, these eco-friendly polymers are less widespread and studied than BPA-PCs for electronic applications. Herein, in this work composites consisting of a CO_2-derived poly(cyclohexene)carbonate (PCHC) polymer matrix loaded with different weight percentages of reduced graphene oxide (rGO) and carbon black (CB) have been prepared, and their thermoresistive (TR) characteristics have been evaluated. The prepared composites show enhanced thermal stability but decreased mechanical properties with the incorporation of the filler, regardless of its type and loading, compared to the neat polymeric matrix. With respect to the electrical conductivity, PCHC composites show values comparable to those of BPA-PCs, representing therefore a suitable replacement for electronic applications. TR characterization has been performed on the 5.0rGO and 4.0CB composites, reaching sensitivities (S) up to $S_{40°C-100°C} = -1.3 \times 10^{-4} °C^{-1}$ for 5.0rGO and $S_{40°C-100°C} = 6.5 \times 10^{-5} °C^{-1}$ for the 4.0CB composite. This work demonstrates the suitability of PCHC/rGO and PCHC/CB composites for TR sensing applications, opening a path towards environmentally friendlier electronic solutions.

1 | Introduction

The interconnectivity provided by the Internet of Things (IoT) has enabled the digital transition of modern society, allowing the ubiquitous exchange of data through wired or wireless communication [1]. The fast and large-scale production of smart electrical and electronic equipment (EEE) has at the same time shortened product lifespan. Devices are in many cases replaced before their actual end of life (EoL) due to programmed obsolescence, accelerating the increasing generation of electronic waste (e-waste) [2]. E-waste has a negative environmental impact, since EEE is composed of a diverse range of materials (e.g., gold, Cu, and rare metals; Pb, As and halogenated hazardous components and polystyrene or polycarbonate polymeric materials [3]). This material diversity is the core of the complicated recyclability of electronic components at their EoL [4].

In order to address the e-waste problem, there is a strong interest in the development of advanced sustainable polymeric matrices or binders for the manufacturing of sensors. Sustainable polymeric materials incorporate properties such as degradability, recyclability, or reusability and, when loaded with electrically conductive

Highlights

- Green PCHC polymer was loaded with rGO and CB for thermosensitive applications.
- PCHC composites show comparable electrical results to conventional BPA-PCs.
- Percolation threshold values ≈2.3 wt.% rGO and 1.5 wt.% CB were obtained.
- Thermoresistive sensors were developed for sustainable electronics.

carbonaceous fillers, can be explored for the manufacturing of eco-friendly conducting materials for electrical applications [5].

High-performance polymers, such as bisphenol A polycarbonates (BPA-PCs), possess high mechanical strength, impact, and thermal resistance properties which could be tuned depending on the synthesized PC grade or blend. These properties have permitted the exploration of this polymer in engineering and daily consumer applications. In the specific case of electronics, BPA-PCs are found in mobile phone casings, computers, game consoles, and DVD/CDs data storage devices, among others [6]. Besides, their transparency and conformability enable them to be explored as substrates for printed conformable/transparent electronics applications [7].

The downside concerning BPA-PCs is the chemicals involved in their synthesis. BPA-PCs are commonly synthesized by the polycondensation reaction between bisphenol A (BPA) and phosgene ($COCl_2$) [6]. The former is a precursor used in the synthesis of BPA-PCs, but studies warn about its harmful effects [8] while the latter, phosgene, is highly toxic [9]. Literature reports alternative synthesis pathways for obtaining carbonate (—O—C=O—O—) monomeric units by replacing phosgene gas [10] with diphenyl carbonate [11]. Even though the aforementioned synthesis route eliminates the use of phosgene, BPA is still required.

The carbonate moiety could be achieved following a BPA free synthesis based on the reaction between epoxides and carbon dioxide (CO_2), producing carbon dioxide derived polycarbonate (CO_2-PCs) [12]. Environmental problems associated with CO_2 emissions have been reported for several years, and their impact is expected to increase in the coming years. To mitigate the impact of greenhouse gases, significant efforts have been directed towards decoupling polymer production from petrochemical resources [13]. Upcycling CO_2 feedstock and incorporating it as a chemical reagent promotes polymer green synthesis and presents advantages by reducing the environmental impact of this gas and avoiding the use of hazardous chemicals. It should be mentioned that CO_2-PCs are aliphatic, whereas BPA-PCs are aromatic. This fact has an impact on the physical–chemical properties of the polymer and, therefore, on its functional response.

BPA-PCs have been studied as active materials combined with electrically conductive carbonaceous fillers for the production of sensors, such as piezoresistive sensors [14, 15]. Different strategies could be followed to promote low environmental impact digitalization, such as producing composites using green solvents, low-impact binders, or reused fillers among other options. In the present case, the use of a more sustainable PCHC binder has been explored. PCHC has been loaded with carbonaceous nanofillers, commonly studied such as carbon nanotubes (CNTs), graphene (G), or carbon black (CB) [16]. CNTs are 1D materials usually used due to their high aspect ratio, meaning that an electrically conductive composite can be achieved at a low filler loading [17]. In contrast, 2D or 3D materials like reduced graphene oxide (rGO) or CB typically require higher loadings, with the latter requiring the highest. The effect of increasing the dimension of the filler also affects the functional response of the composite.

The percolation threshold (P_c), defined as the concentration at which the composite experiences an increase of several orders of magnitude in the electrical conductivity [18], is studied through percolation theory. The transition from an insulating matrix to a conductive composite can be divided into three zones. The first zone consists of the insulating region, where the amount of filler incorporated into the matrix is too low. Even though the electrical conductivity is slightly higher than that of the neat polymer, the amount of filler is not enough to produce interconnected conductive paths. In the second zone, an "*S*-shape" graph is obtained. The continuous inclusion of filler induces an increase of several orders of magnitude in the electrical conductivity as connected paths are formed, meaning that the P_c is reached. The final, third zone is the conductive zone, characterized by a plateau. In this saturation zone, further addition of filler does not induce significant changes in the electrical conductivity of the composite [19].

Thermoresistive sensors evaluate temperature variations through changes in the electrical resistance of the material [20]. In this sense, the thermal properties of the composites, such as those measured by TGA or DSC, as well as their electrical properties, are required to select the most promising sample. Also, SEM and FTIR techniques are required, as the nanofiller distribution within the matrix could alter the electrical properties. Overall, these types of temperature sensors are classified into resistance temperature detectors (RTDs) or thermoresistors. In the first case, devices are composed of metals such as platinum (Pt), while the latter rely on ceramic materials [21]. Even though there is a broad range of sensors in this field, their fabrication is generally energetically demanding and involves toxic materials [22]. The exploration of carbon dioxide derived poly(cyclohexene)carbonate (PCHC) as a binder offers a sustainable alternative to conventional rigid temperature sensors by reducing the use of metals and ceramics associated with mining and refining [7].

In this research, a PCHC matrix has been loaded with varying weight percentages of two electrically conductive fillers, rGO and CB, in order to obtain thermoresistive sensors. Physicochemical characterizations of the prepared films have been conducted, and the most promising samples were subsequently evaluated in terms of their functional performance.

2 | Experimental Section

2.1 | Reagents

Commercial PCHC with the reference QPAC 130 was purchased as pellets from Empower Materials, New Castle USA. The chemical properties of the polymer include a molecular weight in the

range of 150.00–200.00, a density of 1.10 g cm^{-3}, an estimated decomposition onset temperature of 250°C, and a glass transition temperature of T_g = 120°C–130°C.

Two conductive carbon nanofillers have been selected for composite preparation: rGO and CB. The former has been acquired from LayerOne, with a thickness of 1 nm per layer, a flake size of 5 μm, a surface area of 300–350 m^2 g^{-1}, annealed at 1100°C, an apparent density of 0.038–0.041 g cm^{-3}, and a powder compact electrical conductivity of 7 S cm^{-1}. CB Vulcan XC 72R, with a particle diameter of 20–30 nm, bulk density of ≈0.0961 g cm^{-3}, and a specific surface area of 18–550 m^2 g^{-1}, was purchased from Delta Tecnic S.A. The polymer and nanofillers were prepared by solvent casting using dichloromethane (DCM) which was supplied by Sigma Aldrich.

2.2 | Composite Film Processing

PCHC polymer and the nanocomposites were prepared by the solution casting method. A 16 wt.% PCHC solution (2 g of polymer in 8 mL of solvent) was magnetically stirred in DCM for 1 h at room temperature (RT). Composites were prepared by first dissolving 2 g of PCHC in 4 mL of DCM solvent. Then, in a separate vial, different wt.% amounts of rGO or CB were dispersed in 4 mL of DCM. The solution was bath ultrasonicated using an ATU series ATM ultrasonic bath with a power of 220 W for 3 h at a controlled temperature between 25°C and 30°C before being added to the previously prepared polymeric solution. The resulting PCHC-filler solution was magnetically stirred for an additional hour at RT. Finally, the solution was poured onto a glass surface, and films were prepared using the Dr. Blade equipment. Films were dried overnight at RT to ensure complete solvent evaporation, obtaining an average thickness of ≈0.137 ± 0.04 mm. The wt.% of each filler added to the polymers, as well as the nomenclature that will be used throughout this work, is listed in Table 1.

2.3 | Sample Characterization

Morphological characterization of rGO and CB was examined using a Hitachi S-4800 SEM instrument, obtaining the images at an accelerating voltage of 5.0 kV. Additionally, CB was analyzed with transmission electron microscopy (TEM) using a JEOL JEM 1400 Plus (JEOL, Japan) instrument at an accelerating voltage of 100 kV. Filler sizes were analyzed with ImageJ software.

TABLE 1 | List of the prepared composites indicating the nomenclature and wt.% of filler added to the PCHC polymeric matrix.

Carbonaceous fillers	Wt.%	Nomenclature
Reduced graphene oxide (rGO)	0.5; 1.0; 1.5; 2.5; 3.0; 4.0; 5.0	0.5rGO; 1.0rGO; 1.5rGO; 2.5rGO; 3.0rGO; 4.0rGO; 5.0rGO
Carbon black (CB)	1.0; 1.5; 2.0; 2.5; 3.0; 4.0	1.0CB; 1.5CB; 2.0CB; 2.5CB; 3.0CB; 4.0CB

Infrared spectra were collected with a Nicolet Nexus FTIR spectrophotometer (Thermo Electron Corporation). The FTIR spectra were obtained using an ATR accessory in the range of 400 to 4000 cm^{-1} at a resolution of 4 cm^{-1} and 32 scans per spectrum.

The thermal stability of the composites was evaluated twice for the same sample using thermogravimetric analysis (TGA) in an SDT Q 600 TA instruments thermobalance. Five milligrams of the samples were subjected to heating from 25°C to 800°C at a heating rate of 10°C min^{-1} under a nitrogen atmosphere. The maximum degradation temperature (T_{Dmax}) was calculated from the minimum of the first derivative curves. Thermal transitions were determined using a Water TA DSC25 discovery Differential scanning calorimeter (DSC). Ten milligrams of each sample were sealed in aluminium pans and subjected to a heating run from −70°C to 150°C at a scanning rate of 10°C min^{-1} under a constant nitrogen flow (20 mL min^{-1}). For each composite, glass transition temperatures ($T_{g\text{-}onset}$, $T_{g\text{-}endset}$) were identified. In both techniques, the average values of two measurements are presented.

Mechanical properties were tested in tensile mode using a Shimadzu model AG-IS universal testing machine with a load cell of 500 N. Samples with rectangular dimensions of approximately 10 mm × 50 mm × ≈0.14 mm were measured at a test velocity of 1 mm min^{-1}. The shown results are the average values of three measurements for each sample.

RT DC electrical conductivity was measured with a Keithley 487 picoammeter/voltage source. Measurements were performed at different points on the sample from −10 V to +10 V with a step of 1 V. Before the measurement, 5 mm diameter gold round electrodes were sputtered on both sides of the samples using a Quorum Q150T S sputter coater. The electrical conductivity of the composites was calculated as the inverse of the resistivity (ρ), obtained from the resistance (R) determined from the I–V results, following Equation (1), where L is the thickness of the sample, and A is the area of the electrodes.

$$\sigma = \frac{1}{\rho} = \frac{L}{RA} \tag{1}$$

2.4 | Thermoresistive Functional Characterization

The thermoresistive response was evaluated in the 4.0CB and 5.0rGO composites using an Agilent 34401A multimeter synchronized with a Linkam THMSE600 temperature oven. Silver ink (Agar Scientific, reference AGG3790) was used as a parallel conductive electrode in surface mode (10 × 10 mm, electrode length × distance between them). Electrical contact with the multimeter was achieved with copper wires.

The heating–cooling cycles were divided into cycles ranging from 30°C to 45°C at 5°C min^{-1} and from 40°C to 100°C at 10°C min^{-1} for both composites. The thermoresistive sensitivity (S) was determined according to Equation (2):

$$S = \frac{\Delta R / R_0}{\Delta T} \tag{2}$$

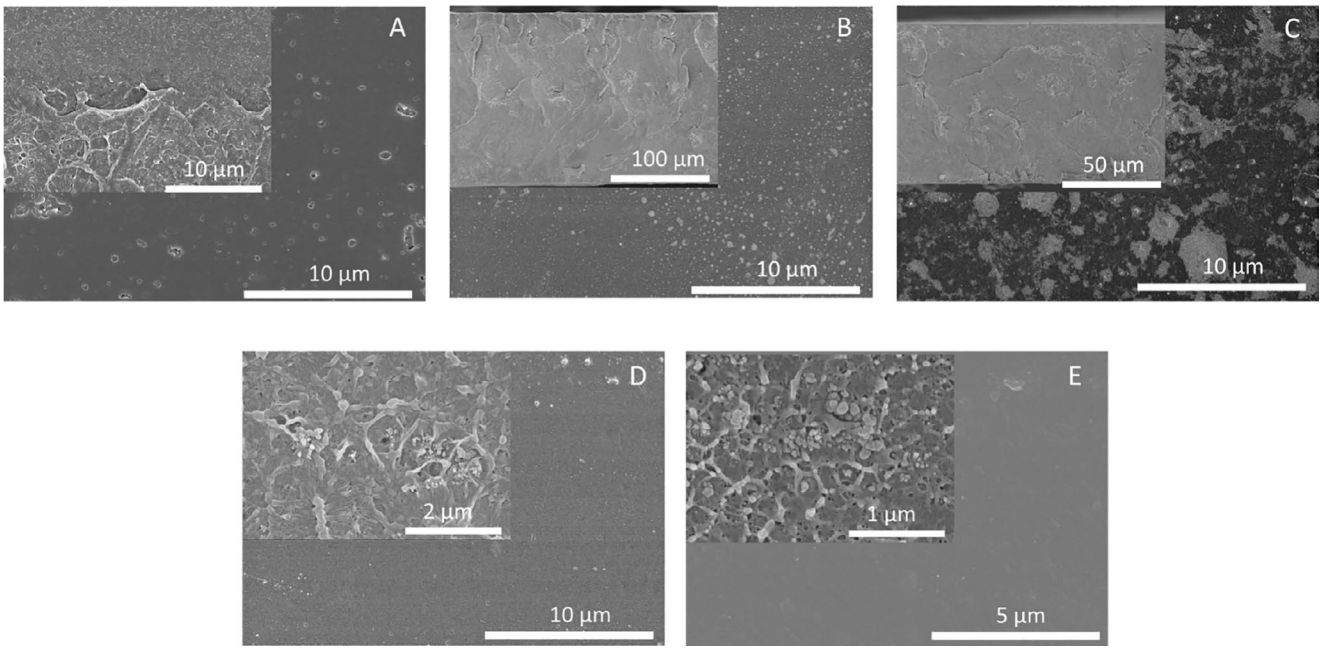

FIGURE 1 | SEM images of the surface and cross-section (inset) of (A) PCHC matrix and composites containing different wt.% of carbonaceous filler: (B) 1.5rGO, (C) 3.0rGO, (D) 0.5CB and (E) 3.0CB.

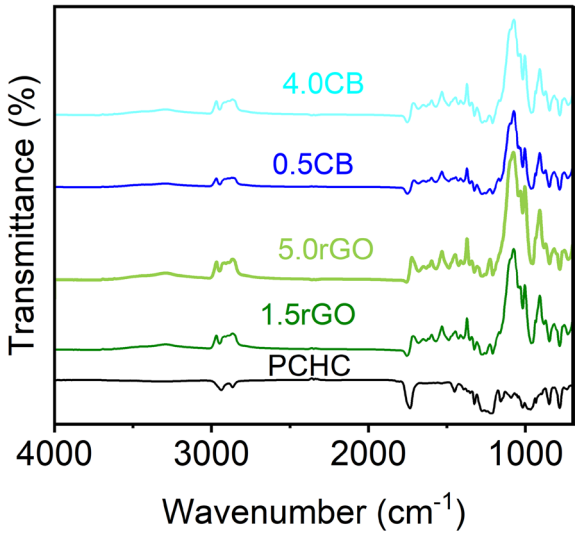

FIGURE 2 | ATR-FTIR spectra of PCHC (black) and corresponding composites prepared at the lowest and highest filler concentrations.

where ΔR and R_0 are the electrical resistance variation and the initial resistance (in Ω), respectively, and ΔT is the temperature variation (in °C).

3 | Results and Discussion

3.1 | Morphological and Chemical Characteristics

Nanofillers distribution within the PCHC polymer matrix was analyzed by SEM, using both surface and cross-section (insets) images, as shown in Figure 1. Pure PCHC polymeric matrix (Figure 1A) exhibits a flat and compact morphology even though some voids and loose areas appear due to solvent evaporation. Filler distribution within the polymeric matrix was analyzed in composites with wt.% below and above the percolation threshold (P_c), as discussed below.

The presence of rGO, a 2D nanofiller, is associated with white platelet-like structures. Increasing the amount of filler from 1.5rGO (Figure 1B) to 3.0rGO (Figure 1C) results in a flatter and more compact surface [23]. The distribution of CB, a 3D nanofiller, is associated with its spherical geometry [24]. At 0.5CB Figure 1D, several spheres are observed forming small agglomerates, while at 3.0CB, interconnected agglomerates are distributed throughout the polymeric matrix.

FTIR analysis, Figure 2, allows us to evaluate the characteristic bands of the polymer and possible polymer/nanofiller interactions. The characteristic PC bands are observed at 1756 cm^{-1} (carbonyl [C═O] peak) [25], at 1015 cm^{-1} (—C—O—C— symmetric stretching); at 1158 and 1220 cm^{-1} (—C—O—C asymmetric stretching); at 1079 cm^{-1} (—CH_3 bending) and at 2871 and 2953 cm^{-1} (C—H stretching) [14, 26]. In addition, the bands corresponding to rGO have been reported at 1178–1073 cm^{-1} for C—O epoxide groups, 1620 cm^{-1} for skeletal C═C stretching of alkene groups, and 1723 cm^{-1} for the C═O carbonyl group [27], while for CB the characteristic bands appear at 1739 cm^{-1} (C═O), 1578 cm^{-1} (C—O), and 1365 cm^{-1} [28]. Possible shifts in the spectra due to filler incorporation were analyzed in composites loaded with the lowest and highest filler contents, which were considered representative of all prepared samples. No new peaks or peak shifts were observed, concluding that there is no chemical bonding between the polymer and the fillers.

Petrochemical BPA-PCs possess two aromatic benzene rings, whose presence is reflected in the FTIR spectra by the C═C stretching band at around 1242 cm^{-1} [29]. In contrast, the absence of this

peak in PCHC confirms its aliphatic nature. These structural differences could influence the thermal and mechanical properties of each polymer.

3.2 | Thermal Properties

Thermal properties have been analyzed to select an appropriate working temperature range for the subsequent thermoresistive analysis. The results obtained from the thermal analysis have been collected in Table 2.

TABLE 2 | Average thermal characteristics of the pure matrix and the composites.

Composite wt.%	TGA	DSC	
	T_{dmax} (°C)	$T_{g\text{-onset}}$ (°C)	$T_{g\text{-endset}}$ (°C)
0	283.7 ± 0.2	91.4 ± 12.6	97.4 ± 13.7
1.5rGO	309.2 ± 18.1	91.7 ± 4.9	98.7 ± 1.0
3.0rGO	315.8 ± 5.4	90.5 ± 13.6	94.6 ± 11.0
5.0rGO	325.8 ± 1.9	99.6 ± 8.6	106.4 ± 9.0
1.5CB	295.5 ± 12.2	97.8 ± 2.7	104.6 ± 5.1
3.0CB	298.0 ± 4.7	96.8 ± 6.9	101.7 ± 7.0
4.0CB	319.0 ± 12.6	105.3 ± 1.6	111.6 ± 4.1

Note: T_{dmax} has been determined from the first derivative and T_g from the initial ($T_{g\text{-onset}}$) and final ($T_{g\text{-endset}}$) transition temperatures.

The TGA thermograms are presented in Figure 3. The PCHC matrix exhibits a pronounced degradation step of approximately 70% and a maximum degradation temperature of ≈283.7°C ± 0.2°C, which has been attributed to the rupture of carbonyl groups [30]. The composites, Figure 3A for rGO and Figure 3B for CB, also display a single degradation step. In addition, the T_{dmax} values of the composites shifted to slightly higher temperatures compared with those of the PCHC matrix, indicating that filler incorporation enhances thermal stability [31] due to electrostatic surface interactions between the polymer and the fillers.

DSC results are shown in Figure 4A,B. In all cases, the DSC thermograms are characterized by a single thermal event: the glass transition of the polymer. PCHC exhibits a glass transition (T_g) at 91.4°C ± 12.6°C and 97.4°C ± 13.7°C, identified as $T_{g\text{-onset}}$ and $T_{g\text{-endset}}$ respectively, which are consistent with the published literature [32]. Analogously to the TGA measurements, increasing the CB filler content (Figure 4B) leads to a shift in T_g towards higher temperatures, as reported in the literature [33]. The increase in the T_g with filler addition may be attributed to polymer–filler interactions, which reduce segmental mobility. An increase in conductive filler content in polymer matrices decreases their chain mobility and promotes a conductive network in composites, leading to an increase in the T_g of the composites. Nevertheless, for the rGO composites (Figure 4A), there is no significant T_g shift compared to PCHC due to their larger size and smaller surface area (flake size of 5 μm, surface area of 300–350 $m^2 g^{-1}$) compared to CB (particle diameter of 20–30 nm, specific surface area: 18–550 $m^2 g^{-1}$).

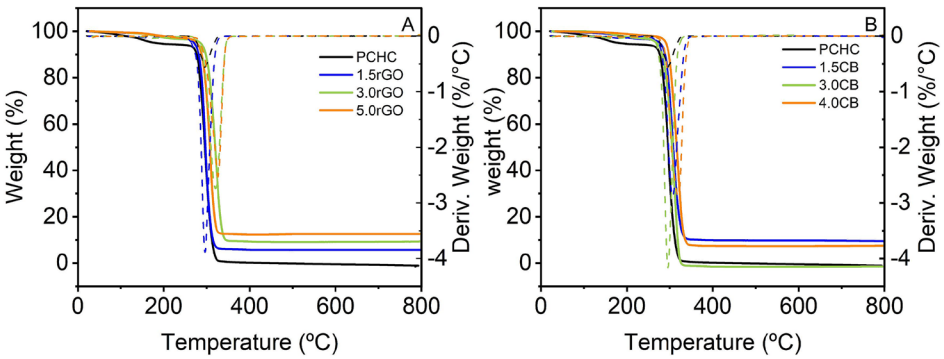

FIGURE 3 | TGA thermograms representing mass percentage (solid line, left axis) and the first derivative (dashed lines, right axis) for (A) rGO and (B) CB filler loaded composites.

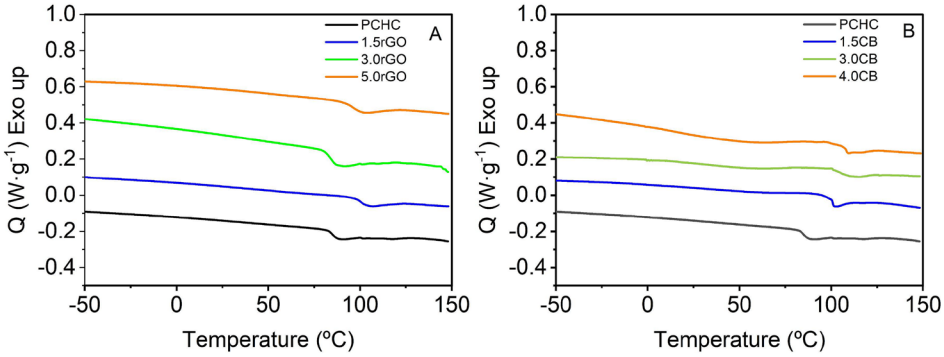

FIGURE 4 | DSC thermograms of the pristine PCHC matrix and composites loaded with different amounts of (A) rGO and (B) CB.

The synthesis of PCs, whether based on BPA or CO_2, leads to different thermal properties. The thermal degradation of BPA-PCs is reported at 400°C, whereas T_g values range from 140°C to 150°C [34–36]. Furthermore, literature reports $T_g \approx 11$°C and 22°C and thermal degradation ≈210°C and 253.9°C for the linear CO_2-PCs poly(ethylene)carbonate (PEC) and poly(propylene)carbonate (PPC), respectively [37, 38]. Therefore, the chemical structure impacts the thermal properties, which are lower for cyclic PCHC than for BPA-based polycarbonates, but improved compared with linear aliphatic CO_2-PCs.

3.3 | Mechanical Properties

Representative uniaxial mechanical stress–strain curves for PCHC and the corresponding composites with rGO and CB are shown in Figure 5A,B. From each stress–strain curve, the Young's modulus (E) and maximum strain (ε_{max}) have been determined. The overall mechanical properties of PCHC critically depend on the block composition [39], polymerization conditions [40] or catalyst processes [41] as well as on the filler type and content in the composites.

PCHC exhibits brittle behavior with $\varepsilon_{max} \approx 2.3\%$ and $E \approx 1521.8 \pm 850.0$ MPa, which are values within the range reported in the literature [42]. Comparing the measured mechanical properties of this work with bibliography results for BPA-PCs [43, 44], Young's modulus values above 2000 MPa have been measured for standard petrochemical PCs. The developed PCHC matrix shows overall lower mechanical properties than BPA-PCs due to the different chemical structure. Nevertheless, the obtained values are suitable for a large range of applications, including electronics.

Independently of the filler type, the same tendency is preserved in the composites, as shown in Figure 5C,D. As the filler content increases, both Young's modulus (E) and elongation at break (ε_b) decrease compared to the pure PCHC matrix. These results are consistent with the chemical analyses, as no chemical interactions exist between the filler and the polymer matrix. Thus, at low filler contents, the filler first acts as reinforcements of the polymer matrix, whereas at higher filler contents, they act as defect sites that promote mechanical failure. Finally, the measured behavior and the differences observed among the composites have been attributed to variations in filler aspect ratio, agglomerates, voids/breakages, and filler dispersion inside the matrix, which act as defects.

3.4 | Electrical Properties

Electrical conductivity was calculated from the slope of the linear I-V curves (Figure 6A,B) following Equation (1). PCHC is an insulating matrix with an electrical conductivity in the order of $\approx 10^{-11}$ S m^{-1}. The incorporation of electrically conductive carbonaceous nanofillers, such as rGO or CB, is a well-known strategy to transform an insulating polymeric matrix into electrically conductive composites, opening the possibility of studying these materials as thermoresistive sensors. In most samples, a linear ohmic behavior was observed, with a slight loss of linearity at filler wt.% near and above the percolation threshold (P_c) due to interfacial polymer–filler contributions [45].

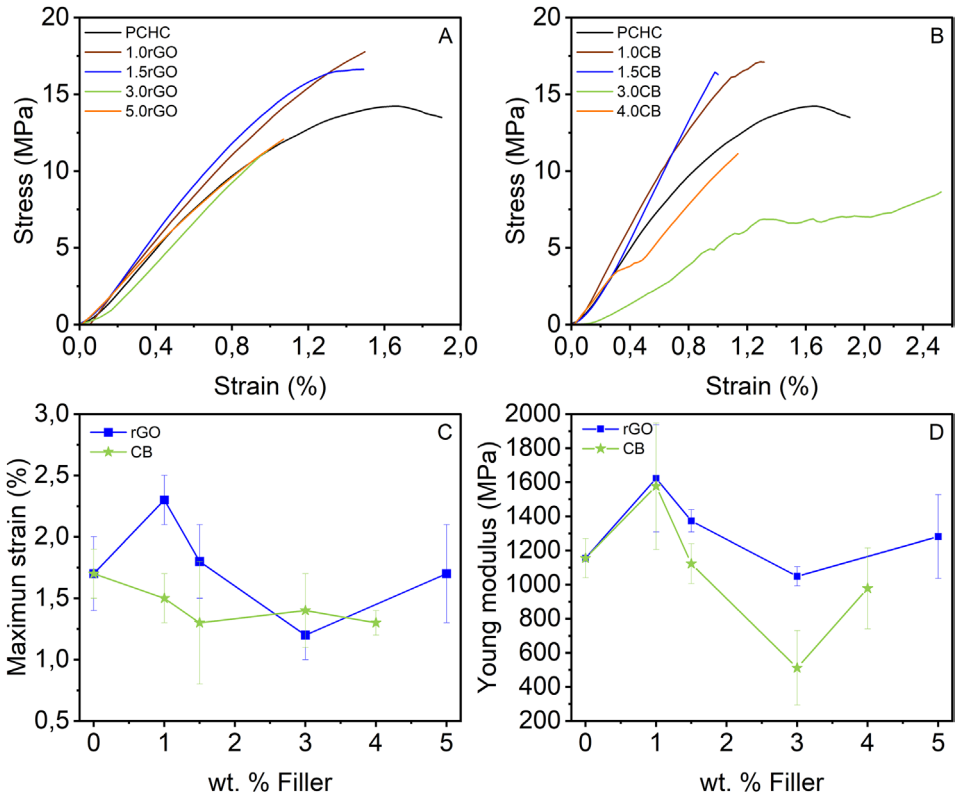

FIGURE 5 | Average stress–strain curves for (A) rGO and (B) CB composites. Mechanical parameters extracted from the previous curves: (C) maximum strain and (D) Young's modulus.

Beginning with the rGO loaded composites shown in Figure 7A (blue line), an electrical conductivity variation of two orders of magnitude was calculated from the pure PCHC matrix to the 2.5rGO composite ($\sigma \approx 5.94 \times 10^{-9}\,S\,m^{-1}$), followed by a sharp increase of approximately 7 orders of magnitude for the 3.0rGO composite ($\sigma \approx 0.07\,S\,m^{-1}$). A similar behavior is observed for the CB composites shown in Figure 7A (green line), with an electrical conductivity variation of one order of magnitude for the 1.5CB composite ($\sigma \approx 9.71 \times 10^{-10}\,S\,m^{-1}$) with respect to the pure PCHC polymer and an increase of about 8 orders of magnitude for the 2.0CB ($\sigma \approx 0.078\,S\,m^{-1}$) composite. Films loaded with the highest filler concentrations, 5rGO and 4.0CB, show similar maximum electrical conductivities of $\sigma \approx 0.22\,S\,m^{-1}$ and $\sigma \approx 0.18\,S\,m^{-1}$, respectively, which are comparable to those reported for multiwalled carbon nanotubes (MWCNTs)-reinforced PCHC composites [46].

The observed electrical conductivity variations of several orders of magnitude at a given filler concentration are associated with a percolative behavior. The percolation threshold (P_c) and critical exponent (t) were determined using Equation (3), where P corresponds to the filler loading in wt.% and t depends on filler type and geometry. In Figure 7B, a linear relationship is observed, from which P_c and t values are extracted.

$$\sigma = \sigma_0 \left(P - P_c\right)^t \tag{3}$$

For rGO, $P_c = 2.3$ wt.% and $t = 0.7$, whereas for CB, $P_c \approx 1.5$ wt.% and $t \approx 0.5$ have been obtained. Despite the critical exponent t being 1.30 for 2D and 2.0 for 3D networks, deviations from these values have also been reported [47]. The obtained P_c and t values are similar to those reported for BPA-PC/carbonaceous filler composites. For rGO, a 2D filler, different P_c values have been reported depending on the graphene type and composite processing methods. For example, polycarbonate/expanded graphite composites show $P_c \approx 1.08$ wt.% and $t \approx 2.2$, while polycarbonate/graphene nanoplatelet composites show $P_c \approx 4$ wt.% [48, 49]. In the case of CB, at least 14 wt.% of CB has to be added (critical t exponent value of ≈2.9) to BPA-PCs to obtain a conductive composite [36].

In general, 2D carbonaceous fillers require lower addition of material compared to 3D fillers to reach the percolation threshold [50]. The electrical properties of the composites depend on the filler aspect ratio, dispersion, geometry, distribution, and agglomeration [50], among others. These parameters influence both the maximum electrical conductivity and the P_c value. The distribution of the filler within the polymer matrix can result in lower P_c values for PC/CB composites, such as 3.6 or 1.38 wt.% with $t = 0.33$ for CB [51, 52] as reported in this work. In order to support our results, TEM images of CB filler are presented in Figure S1, where the measured P_c values could be attributed to the presence of agglomerates and the observed anisotropic filler structures. This effect is also observed in the previously described SEM images (Figure 1D,E).

Based on these results, PCHC composites (whether loaded with rGO or CB) exhibit P_c and maximum electrical conductivities

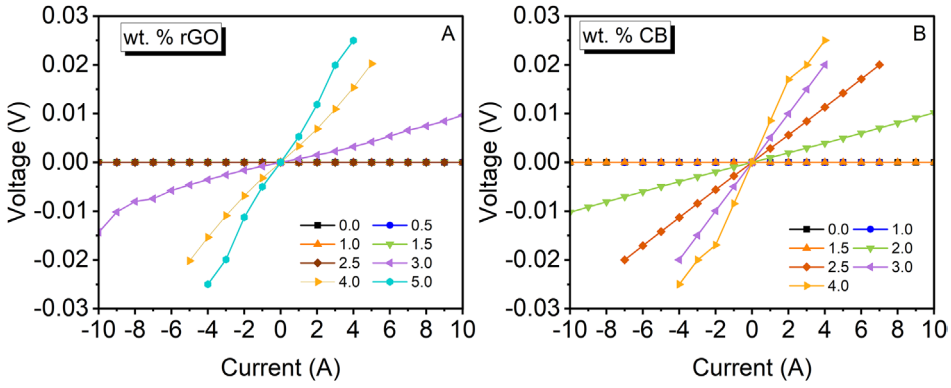

FIGURE 6 | Representative I–V curves for the pristine polymer and composites with different filler contents of (A) rGO and (B) CB.

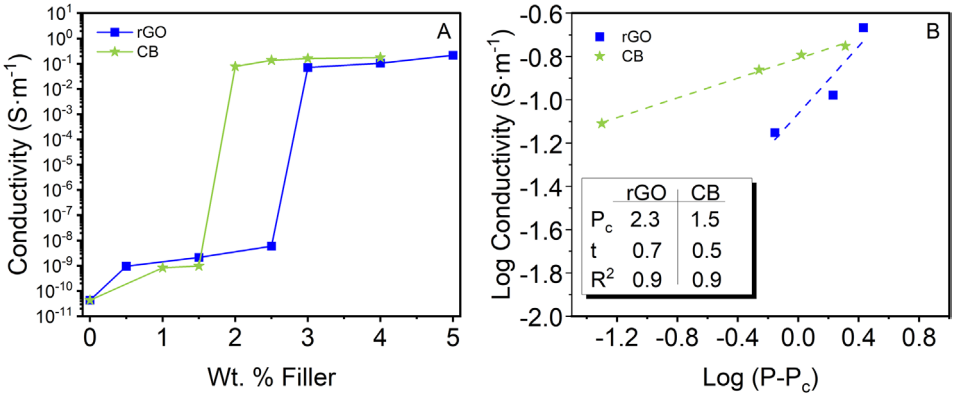

FIGURE 7 | (A) Electrically conductivity as a function of filler concentration for both rGO and CB composites and (B) calculation of P_c and t parameters based on previous electrical conductivity data.

comparable to those reported for BPA-PC/carbonaceous filler composites. In other words, when only electrical conductivity is considered, the choice of polymer could be guided by its more sustainable profile. However, when specific functionality is required, additional physical properties must be considered. In the specific case of thermoresistive applications, the thermal properties of the composites are particularly relevant.

3.5 | Thermoresistive Response

In the scope of sustainable digitalization, CO_2-PCHC composites could serve not only as conductive tracks due to their high electrical conductivity, but also as sustainable thermoresistive sensing materials. The performance of a thermoresistive sensor is quantified by its sensitivity (S), which, in the present case, depends on filler concentration, polymer/filler interactions, filler dispersion/agglomeration, and the temperature range, among other parameters [53, 54]. In fact, the possibility of obtaining both positive and negative sensitivity values with electrically conductive fillers such as CNTs, G, or CB has already been reported [55, 56].

The incorporation of CNTs into a PCHC matrix for thermoresistive applications has been reported. PCHC composites containing 3.0 wt.% MWCNTs exhibited sensitivities of $S \approx -1.3 \times 10^{-4}\,°C^{-1}$ within 40°C–100°C and 30°C–45°C temperature ranges [46]. In the present work, the 5.0rGO and 4.0CB samples have been selected owing to their improved thermal and electrical properties among the prepared samples. In the case of the 5.0rGO sample, the electrical resistance during temperature cycling (Figure 8A) varies inversely to temperature variation for the low and high temperature intervals (35°C to 40°C, representative of human body temperature, and 40°C to 100°C for higher temperature applications). Although a suitable thermoresistive correlation is observed, tests performed over the wider temperature range reveal a non-linear features near 75°C–80°C, which may be related to sub-T_g relaxation processes temperature [25]. The thermoresistive sensitivities for rGO are shown in Figure 8B, with values of $S_{35-40} = -2.4 \times 10^{-4} °C^{-1}$ and $S_{40-100} = -1.3 \times 10^{-4} °C^{-1}$. Larger temperature changes show higher sensitivity in comparison with the literature [57]. The results for the CB composite at both temperature ranges are shown in Figure 8C. Under similar conditions, a consistent relationship between electrical resistance and temperature variation is observed after four thermal cycles. The sensitivity of the CB composite, $S_{35-40} = 3.3 \times 10^{-4} °C^{-1}$ and $S_{40-100} = 6.5 \times 10^{-5} °C^{-1}$, Figure 8D, follows a similar trend as for the rGO composite with higher sensitivity observed at elevated temperatures. Both composites have shown similar sensitivity values on the order of $\approx 10^{-4} °C^{-1}$ in the 40°C–100°C temperature range, demonstrating their potential for temperature sensing based on their thermoresistive response.

Few studies have been reported, up to our knowledge, concerning petrochemical polycarbonates for thermoresistive sensors. Therefore, the obtained results have been compared with previously reported sustainable polymer/carbonaceous filler composites. Bio-based photocurable biopolymers loaded with 6 wt.% MWCNTs have shown a $S = 0.43$ in the temperature range of 25°C–50°C [23], while a PCL polymer matrix loaded with rGO shows $S \approx 5.22\%$ to 5.55% per °C [58]. Comparable results have been obtained for a water soluble HPC matrix loaded with 4.0/1.0 multiwalled CNTs/fullerene fillers, showing $S \approx (1.6 \pm 0.2) \times 10^{-4} °C^{-1}$ and $(2.4 \pm 0.3) \times 10^{-4} °C^{-1}$ in the

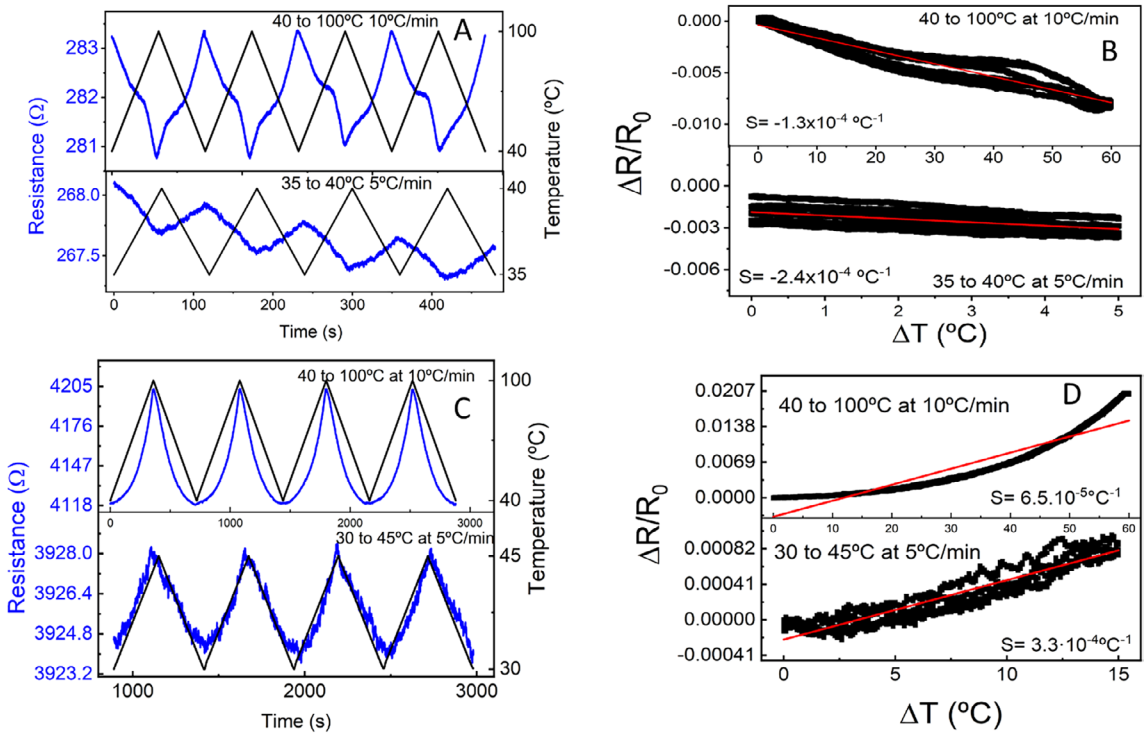

FIGURE 8 | Functional thermoresistive response measured over two temperature ranges. The left column shows the four measured thermal cycles, whereas the right columns show the sensitivity calculated from these cycles. Functional performance corresponding to (A and B) 5rGO and (C and D) 4.0CB composites.

30°C–50°C and 50°C–100°C temperature intervals, respectively [59]. Thus, despite the relatively low sensitivity measured in the present work, the proposed thermoresistive sensor, consisting of a robust and eco-friendly polymer binder, demonstrates potential for sustainable electronic applications.

4 | Conclusions

Carbon dioxide derived PCHC polymer matrices loaded with rGO and CB conductive fillers have been developed for thermoresistive sensing applications. Overall, the prepared composites showed enhanced thermal stability but decreased mechanical properties (E and ε_b) with increasing wt.% of rGO and CB compared to the pure PCHC polymer matrix. Regarding the electrical properties, percolation threshold values of ≈2.3% wt. for rGO and 1.5% wt. for CB have been calculated and maximum electrical conductivities of $\sigma \approx 0.22$ and $0.18\,S\,m^{-1}$ for 5.0rGO and 4.0CB, respectively have been obtained. In addition to this, electrical conductivity values comparable to those reported for BPA-PC/carbon nanofiller composites have been measured, accompanied by an important reduction of the environmental impact in the case of the composites measured in this work. Functional characterization has been conducted on the 5.0rGO and 4.0CB composites, which were selected as the most suitable candidates due to their highest electrical conductivity. Their thermoresistive performance has been quantified by the sensitivity (S), reaching values up to $S_{40°C–100°C} = -1.3 \times 10^{-4} °C^{-1}$ for 5.0rGO and $S_{40°C–100°C} = 3.3 \times 10^{-4} °C^{-1}$ for the 4.0CB composite. Overall, the aspect/ratio of the filler does not affect significantly the performance, with sensitivity values in the order of $10^{-4} °C^{-1}$ for both types of fillers. Herein, this work demonstrates that CO_2-derived polymers, such as PCHC, possess suitable characteristics for the development of sustainable conductive composites for electronic applications, including thermoresistive sensing.

Author Contributions

Nikola Peřinka: conceptualization, methodology, writing – review and editing, supervision, formal analysis. **José Luis Vilas-Vilela:** investigation, supervision, funding acquisition, resources. **Ane Martín-Ayerdi:** investigation, methodology, formal analysis, writing – original draft. **Itziar Oyarzabal:** conceptualization, methodology, writing – review and editing, supervision, resources. **Sergio Merillas:** investigation, formal analysis. **Senentxu Lanceros-Méndez:** conceptualization, methodology, formal analysis, writing – review and editing, project administration, funding acquisition. **Pedro Costa:** investigation, formal analysis, writing – original draft, resources. **Luis Rubio-Peña:** investigation, formal analysis.

Acknowledgments

This study forms part of the Advanced Materials program and was supported by MCIN with funding from European Union NextGenerationEU (PRTR-C17.I1) and (L. R.-P.). The authors thank funding from the Basque Government under the Elkartek and IKUR programs. The authors are grateful to the Fundação para a Ciência e Tecnologia (FCT) for financial Support under the framework of Strategic Funding UID/FIS/04650/2025 (https://doi.org/10.54499/UID/04650/2025) and 2023.07491.CEECIND (10.54499/2023.07491.CEECIND/CP2841/CT0015) (P.C.), and to the Education Department of the Government of the Basque Country (Grupos de Investigación, IT1756-22).

Funding

This study forms part of the Advanced Materials program and was supported by MCIN with funding from European Union NextGenerationEU (PRTR-C17.I1) and (L. R.-P.). The authors thank funding from the Basque Government under the Elkartek and IKUR programs. The authors are grateful to the Fundação para a Ciência e Tecnologia (FCT) for financial Support under the framework of Strategic Funding UID/FIS/04650/2025 (https://doi.org/10.54499/UID/04650/2025) and 2023.07491.CEECIND (10.54499/2023.07491.CEECIND/CP2841/CT0015) (P.C.), and to the Education Department of the Government of the Basque Country (Grupos de Investigación, IT1756-22).

Conflicts of Interest

The authors declare no conflicts of interest.

Data Availability Statement

The data that support the findings of this study are available from the corresponding author upon reasonable request.

References

1. B. X. Chai, M. Gunaratne, M. Ravandi, et al., "Smart Industrial Internet of Things Framework for Composites Manufacturing," *Sensors* 24 (2024): 4852, https://doi.org/10.3390/s24154852.

2. S. P. Grandhi, P. P. Dagwar, and D. Dutta, "Policy Pathways to Sustainable E-Waste Management: A Global Review," *Journal of Hazardous Materials Advances* 16 (2024): 100473, https://doi.org/10.1016/j.hazadv.2024.100473.

3. M. P. Cenci, T. Scarazzato, D. D. Munchen, et al., "Eco-Friendly Electronics—A Comprehensive Review," *Advanced Materials Technologies* 7 (2022): 2001263.

4. K. Magoda and L. Mekuto, "Biohydrometallurgical Recovery of Metals From Waste Electronic Equipment: Current Status and Proposed Process," *Recycling* 7 (2022): 67.

5. P. Martins, N. Pereira, A. C. Lima, et al., "Advances in Printing and Electronics: From Engagement to Commitment," *Advanced Functional Materials* 33 (2023): 2213744.

6. M. Gohil and G. Joshi, "Perspective of Polycarbonate Composites and Blends Properties, Applications, and Future Development: A Review," in *Green Sustainable Process for Chemical and Environmental Engineering and Science: Green Composites: Preparation, Properties and Allied Applications* (Elsevier, 2022), 393–424.

7. Z. Yu, X. Jian, J. Wang, X. Zhang, and S. Zhai, "Advantages and Research Progress of Polycarbonates in Flexible Electronic Devices," *Macromolecular Rapid Communications* (2025): e00705, https://doi.org/10.1002/marc.202500705.

8. A. Tarafdar, R. Sirohi, P. A. Balakumaran, et al., "The Hazardous Threat of Bisphenol A: Toxicity, Detection and Remediation," *Journal of Hazardous Materials* 423 (2022): 127097, https://doi.org/10.1016/j.jhazmat.2021.127097.

9. A. K. Sharma and K. N. Phosgene, "Risk Assessment, Environmental, and Health Hazard," in *Hazardous Gases* (Academic Press, 2021), 313–325.

10. S. Fukuoka, I. Fukawa, T. Adachi, H. Fujita, N. Sugiyama, and T. Sawa, "Industrialization and Expansion of Green Sustainable Chemical Process: A Review of Non-Phosgene Polycarbonate From CO2," *Organic Process Research and Development* 23 (2019): 145–169, https://doi.org/10.1021/acs.oprd.8b00391.

11. H. Wang, F. Xu, Z. Zhang, M. Feng, M. Jiang, and S. Zhang, "Bio-Based Polycarbonates: Progress and Prospects," *RSC Sustainability* 1 (2023): 2162–2179.

12. Y. Liu and X. B. Lu, "Current Challenges and Perspectives in CO2-Based Polymers," *Macromolecules* 56 (2023): 1759–1777.

13. A. A. Yaroslavov, M. S. Arzhakov, and A. R. Khokhlov, "The Life Cycle of Polymer Materials: Problems and Prospects," *Herald of the Russian Academy of Sciences* 92 (2022): 18–24.

14. J. R. Dios, B. Gonzalo, C. R. Tubio, et al., "Functional Piezoresistive Polymer-Composites Based on Polycarbonate and Polylactic Acid for Deformation Sensing Applications," *Macromolecular Materials and Engineering* 305 (2020): 2000379, https://doi.org/10.1002/mame.202000379.

15. P. Costa, J. R. Dios, J. Cardoso, et al., "Polycarbonate Based Multifunctional Self-Sensing 2D and 3D Printed Structures for Aeronautic Applications," *Smart Materials and Structures* 30 (2021): 085032, https://doi.org/10.1088/1361-665X/ac0cbe.

16. Y. Li, X. Huang, L. Zeng, et al., "A Review of the Electrical and Mechanical Properties of Carbon Nanofiller-Reinforced Polymer Composites," *Journal of Materials Science* 54 (2019): 1036–1076.

17. J. Guo, Y. Liu, R. Prada-Silvy, et al., "Aspect Ratio Effects of Multi-Walled Carbon Nanotubes on Electrical, Mechanical, and Thermal Properties of Polycarbonate/MWCNT Composites," *Journal of Polymer Science Part B: Polymer Physics* 52 (2014): 73–83, https://doi.org/10.1002/polb.23402.

18. H. J. Choi, M. S. Kim, D. Ahn, S. Y. Yeo, and S. Lee, "Electrical Percolation Threshold of Carbon Black in a Polymer Matrix and Its Application to Antistatic Fibre," *Scientific Reports* 9 (2019): 6338, https://doi.org/10.1038/s41598-019-42495-1.

19. N. A. Mohd Radzuan, A. B. Sulong, and J. Sahari, "A Review of Electrical Conductivity Models for Conductive Polymer Composite," *International Journal of Hydrogen Energy* 42 (2017): 9262–9273, https://doi.org/10.1016/j.ijhydene.2016.03.045.

20. T. Dinh, H. P. Phan, A. Qamar, P. Woodfield, N. T. Nguyen, and D. V. Dao, "Thermoresistive Effect for Advanced Thermal Sensors: Fundamentals, Design Considerations, and Applications," *Journal of Microelectromechanical Systems* 26 (2017): 966–986, https://doi.org/10.1109/JMEMS.2017.2710354.

21. Z. Song, Z. Chen, G. Du, et al., "Research Progress on Negative Temperature Coefficient Thermistors: Review," *Journal of Materials Science: Materials in Electronics* 36 (2025): 688.

22. V. S. Turkani, D. Maddipatla, B. B. Narakathu, B. J. Bazuin, and M. Z. Atashbar, "A Carbon Nanotube Based NTC Thermistor Using Additive Print Manufacturing Processes," *Sensors and Actuators, A: Physical* 279 (2018): 1–9, https://doi.org/10.1016/j.sna.2018.05.042.

23. C. Mendes-Felipe, P. Costa, I. Roppolo, M. Sangermano, and S. Lanceros-Mendez, "Bio-Based Piezo- and Thermoresistive Photocurable Sensing Materials From Acrylated Epoxidized Soybean Oil," *Macromolecular Materials and Engineering* 307 (2022): 2100934, https://doi.org/10.1002/mame.202100934.

24. L. Campos-Arias, N. Peřinka, P. Costa, J. L. Vilas-Vilela, and S. Lanceros-Méndez, "Stretchable Conductive Inks With Carbon-Based Fillers for Conformable Printed Electronics," *Advanced Engineering Materials* 26 (2024): 2400354, https://doi.org/10.1002/adem.202400354.

25. M. Spyridakou, C. Gardiner, G. Papamokos, H. Frey, and G. Floudas, "Dynamics of Poly(Cyclohexene Carbonate) as a Function of Molar Mass," *ACS Applied Polymer Materials* 4 (2022): 3833–3843, https://doi.org/10.1021/acsapm.2c00299.

26. S. Redjala, N. Aït Hocine, R. Ferhoum, M. Gratton, N. Poirot, and S. Azem, "UV Aging Effects on Polycarbonate Properties," *Journal of Failure Analysis and Prevention* 20 (2020): 1907–1916, https://doi.org/10.1007/s11668-020-01002-9.

27. V. Sharma, Y. Jain, M. Kumari, R. Gupta, S. K. Sharma, and K. Sachdev, "Synthesis and Characterization of Graphene Oxide (GO) and Reduced Graphene Oxide (RGO) for Gas Sensing Application," *Macromolecular Symposia* 376 (2017): 1700006, https://doi.org/10.1002/masy.201700006.

28. I. Islam, S. Sultana, S. Kumer Ray, H. Parvin Nur, M. T. Hossain, and W. Md. Ajmotgir, "Electrical and Tensile Properties of Carbon Black Reinforced Polyvinyl Chloride Conductive Composites," *C* 4 (2018): 15, https://doi.org/10.3390/c4010015.

29. T. T. Li, X. Zhang, Y. Wang, et al., "Carbon Nanotube/Polypropylene/Polycarbonate Conductive Nanocomposite Films: Preparation and Characterization," *Journal of Applied Polymer Science* 138 (2021): 51276, https://doi.org/10.1002/app.51276.

30. D. Wijerathne, Y. Gong, S. Afroj, N. Karim, and C. Abeykoon, "Mechanical and Thermal Properties of Graphene Nanoplatelets-Reinforced Recycled Polycarbonate Composites," *International Journal of Lightweight Materials and Manufacture* 6 (2023): 117–128, https://doi.org/10.1016/j.ijlmm.2022.09.001.

31. M. A. Sohel, A. Mondal, P. M. Arif, S. Thomas, and A. SenGupta, "Effects of Graphene on Thermal Properties and Thermal Stability of Polycarbonate/Graphene Nanocomposite," *Journal of Thermoplastic Composite Materials* 36 (2023): 326–344, https://doi.org/10.1177/0892705721997887.

32. S. D. Thorat, P. J. Phillips, V. Semenov, and A. Gakh, "Physical Properties of Aliphatic Polycarbonates Made From CO2 and Epoxides," *Journal of Applied Polymer Science* 89 (2003): 1163–1176, https://doi.org/10.1002/app.12355.

33. T. Sterzyński, J. Tomaszewska, K. Piszczek, and K. Skórczewska, "The Influence of Carbon Nanotubes on the PVC Glass Transition Temperature," *Composites Science and Technology* 70 (2010): 966–969, https://doi.org/10.1016/j.compscitech.2010.02.013.

34. L. Wang, J. Qiu, and E. Sakai, "Thermal Behavior and Mechanical Properties of Nanocomposites of Polycarbonate Reinforced With Multi-walled Carbon Nanotubes," *Polymer Composites* 38 (2017): E303–E313, https://doi.org/10.1002/pc.23801.

35. F. Y. Castillo, R. Socher, B. Krause, et al., "Electrical, Mechanical, and Glass Transition Behavior of Polycarbonate-Based Nanocomposites With Different Multi-Walled Carbon Nanotubes," *Polymer* 52 (2011): 3835–3845, https://doi.org/10.1016/j.polymer.2011.06.018.

36. V. Brunella, B. G. Rossatto, C. Mastropasqua, F. Cesano, and D. Scarano, "Thermal/Electrical Properties and Texture of Carbon Black pc Polymer Composites Near the Electrical Percolation Threshold," *Journal of Composites Science* 5 (2021): 212, https://doi.org/10.3390/jcs5080212.

37. N. A. Ramlee and Y. Tominaga, "Preparation and Characterization of Poly(Ethylene Carbonate)/Poly(Lactic Acid) Blends," *Journal of Polymer Research* 25 (2018): 54, https://doi.org/10.1007/s10965-018-1451-4.

38. X. Ma, Y. Jiugao, and N. Wang, "Compatibility Characterization of Poly(Lactic Acid)/ Poly(Propylene Carbonate) Blends," *Journal of Polymer Science. Part B, Polymer Physics* 44 (2006): 94–101, https://doi.org/10.1002/polb.20669.

39. G. S. Sulley, G. L. Gregory, T. T. D. Chen, et al., "Switchable Catalysis Improves the Properties of CO2-Derived Polymers: Poly(Cyclohexene Carbonate- b-ε-Decalactone- b-Cyclohexene Carbonate) Adhesives, Elastomers, and Toughened Plastics," *Journal of the American Chemical Society* 142 (2020): 4367–4378, https://doi.org/10.1021/jacs.9b13106.

40. S. Kernbichl and B. Rieger, "Aliphatic Polycarbonates Derived From Epoxides and CO2: A Comparative Study of Poly(Cyclohexene Carbonate) and Poly(Limonene Carbonate)," *Polymer (Guildford)* 205 (2020): 122667, https://doi.org/10.1016/j.polymer.2020.122667.

41. M. Zhang, C. Zhang, P. Zhang, and Z. Liang, "Study of Preparation and Properties of Stereoregular Poly(Cyclohexenylene Carbonate)," *Molecules* 28 (2023): 5235, https://doi.org/10.3390/molecules28135235.

42. C. Koning, J. Wildeson, R. Parton, B. Plum, P. Steeman, and D. J. Darensbourg, "Synthesis and Physical Characterization of Poly(Cyclohexane Carbonate), Synthesized From CO2 and Cyclohexene Oxide," *Polymer* 42 (2001): 3995–4004, https://doi.org/10.1016/S0032-3861(00)00709-6.

43. L. Morales-Zamudio, T. Lozano, F. Caballero-Briones, et al., "Structure and Mechanical Properties of Graphene Oxide-Reinforced Polycarbonate," *Materials Chemistry and Physics* 261 (2021): 124180, https://doi.org/10.1016/j.matchemphys.2020.124180.

44. X. Su, Z. Yang, R. Cheng, et al., "A Comparative Study of Polycarbonate Nanocomposites Respectively Containing Graphene Nanoplatelets, Carbon Nanotubes and Carbon Nanofibers," *Advanced Nanocomposites* 1 (2024): 77–85, https://doi.org/10.1016/j.adna.2023.11.001.

45. J. Wang, S. Yu, S. Luo, B. Chu, R. Sun, and C. P. Wong, "Investigation of Nonlinear I-V Behavior of CNTs Filled Polymer Composites," *Materials Science and Engineering B* 206 (2016): 55–60, https://doi.org/10.1016/j.mseb.2016.01.004.

46. A. Martín-Ayerdi, L. Rubio-Peña, N. Peřinka, et al., "Towards Sustainable Temperature Sensor Production Through CO2-Derived Polycarbonate-Based Composites," *Polymers (Basel)* 16 (2024): 1948, https://doi.org/10.3390/polym16131948.

47. T. Khan, M. S. Irfan, M. Ali, Y. Dong, S. Ramakrishna, and R. Umer, "Insights to Low Electrical Percolation Thresholds of Carbon-Based Polypropylene Nanocomposites," *Carbon (New York)* 176 (2021): 602–631, https://doi.org/10.1016/j.carbon.2021.01.158.

48. A. Gupta and R. K. Goyal, "Electrical Properties of Polycarbonate/Expanded Graphite Nanocomposites," *Journal of Applied Polymer Science* 136 (2019): 47274, https://doi.org/10.1002/app.47274.

49. A. Oyarzabal, A. Cristiano-Tassi, E. Laredo, et al., "Dielectric, Mechanical and Transport Properties of Bisphenol A Polycarbonate/Graphene Nanocomposites Prepared by Melt Blending," *Journal of Applied Polymer Science* 134 (2017): app.44654, https://doi.org/10.1002/app.44654.

50. J. Payandehpeyman and M. Mazaheri, "Geometrical and Physical Effects of Nanofillers on Percolation and Electrical Conductivity of Polymer Carbon-Based Nanocomposites: A General Micro-Mechanical Model," *Soft Matter* 19 (2022): 530–539, https://doi.org/10.1039/d2sm01168a.

51. Y. Li, P. Pötschke, J. Pionteck, and B. Voit, "Electrical and Vapor Sensing Behaviors of Polycarbonate Composites Containing Hybrid Carbon Fillers," *European Polymer Journal* 108 (2018): 461–471, https://doi.org/10.1016/j.eurpolymj.2018.09.027.

52. M. D. Via, J. A. King, J. M. Keith, and G. R. Bogucki, "Electrical Conductivity Modeling of Carbon Black/Polycarbonate, Carbon Nanotube/Polycarbonate, and Exfoliated Graphite Nanoplatelet/Polycarbonate Composites," *Journal of Applied Polymer Science* 124 (2012): 182–189, https://doi.org/10.1002/app.35096.

53. P. Verma, A. Schiffer, and S. Kumar, "Thermo-Resistive and Thermo-Piezoresistive Sensitivity of Carbon Nanostructure Engineered Thermoplastic Composites Processed via Additive Manufacturing," *Polymer Testing* 93 (2021): 106961, https://doi.org/10.1016/j.polymertesting.2020.106961.

54. C. Medina, A. Balam, and F. Avilés, "Thermoresistive Properties of Multilayer Graphene Sheet/Polypropylene Composites Using Four Dissimilar Fillers," *Materials Today Communications* 41 (2024): 110903, https://doi.org/10.1016/j.mtcomm.2024.110903.

55. G. M. Go, S. Park, M. Lim, et al., "Enhanced Positive Temperature Coefficient Intensity and Reproducibility With Synergistic Effect of 0-D and 2-D Filler Composites," *Journal of Materials Science* 57 (2022): 18037–18050, https://doi.org/10.1007/s10853-022-07317-2.

56. C. S. Buga and J. C. Viana, "Development and Characterization of Flexible Carbon Temperature Sensors: A Study on Different Inks and Sensor Designs," *Sensors and Actuators A: Physical* 378 (2024): 115823, https://doi.org/10.1016/j.sna.2024.115823.

57. R. K. Rao, S. Gautham, and S. Sasmal, "A Comprehensive Review on Carbon Nanotubes Based Smart Nanocomposites Sensors for Various Novel Sensing Applications," *Polymer Reviews* 64 (2024): 575–638.

58. P. X. Thinh, C. Basavajara, J. K. Kim, and D. S. Huh, "Characterization and Electrical Properties of Honeycomb-Patterned Poly (E-Caprolactone)/Reduced Graphene Oxide Composite Film," *Polymer Composites* 33 (2012): 2159–2168.

59. F. Avilés, "Thermoresistivity of Carbon Nanostructures and Their Polymeric Nanocomposites," *Advanced Materials Interfaces* 10 (2023): 2300218.

Supporting Information

Additional supporting information can be found online in the Supporting Information section. **Figure S1:** TEM images of carbon black at different magnifications, with scale bars of (A) 500 nm, (B, C) 200 nm, (D, E) 50 nm and (F) 20 nm. White arrows indicate particle and agglomeration sizes.